AD-A168 088

RADC-TR-85-226
In-House Report
February 1986

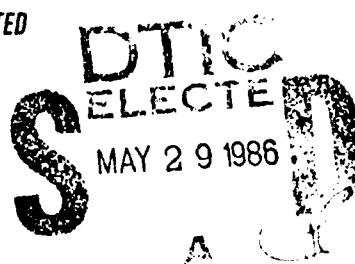# COMPARISON OF MODAL TO NODAL APPROACHES FOR WAVEFRONT CORRECTION

Dr. Donald W. Hanson and Sam E. Fragapane Jr.

APPROVED FOR PUBLIC RELEASE; DISTRIBUTION UNLIMITED

DTIC
ELECTE
S
MAY 2 9 1986
A

ROME AIR DEVELOPMENT CENTER
Air Force Systems Command
Griffiss Air Force Base, NY 13441-5700

This report has been reviewed by the RADC Public Affairs Office (PA) and is releasable to the National Technical Information Service (NTIS). At NTIS it will be releasable to the general public, including foreign nations.
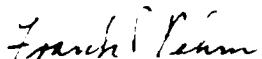
RADC-TR-85-226 has been reviewed and is approved for publication.
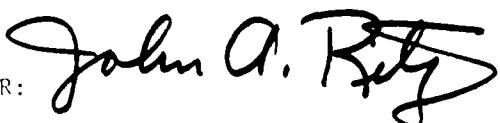
APPROVED: *Thomas G. Pitts*

THOMAS PITTS
Chief, Strategic Surveillance Branch
Surveillance Division

APPROVED: *Frank J. Rehm*

FRANK J. REHM
Technical Director
Surveillance Division

FOR THE COMMANDER: *John A. Ritz*

JOHN A. RITZ
Plans Office

REPORT DOCUMENTATION PAGE

1a REPORT SECURITY CLASSIFICATION			1b RESTRICTIVE MARKINGS		
UNCLASSIFIED			N/A		
2a SECURITY CLASSIFICATION AUTHORITY N/A			3 DISTRIBUTION/AVAILABILITY OF REPORT Approved for public release;		
2b DECLASSIFICATION / DOWNGRADING SCHEDULE N/A			distribution unlimited		
4 PERFORMING ORGANIZATION REPORT NUMBER(S) RADC-TR-85-226			5 MONITORING ORGANIZATION REPORT NUMBER(S) N/A		
6a NAME OF PERFORMING ORGANIZATION Rome Air Development Center	6b OFFICE SYMBOL (If applicable) OCSP		7a NAME OF MONITORING ORGANIZATION N/A		
6c ADDRESS (City, State, and ZIP Code) Griffiss AFB NY 13441-5700			7b ADDRESS (City, State, and ZIP Code) N/A		
8a NAME OF FUNDING/SPONSORING ORGANIZATION Rome Air Development Center	8b OFFICE SYMBOL (If applicable) OCSP		9 PROCUREMENT INSTRUMENT IDENTIFICATION NUMBER N/A		
8c ADDRESS (City, State, and ZIP Code) Griffiss AFB NY 13441-5700			10 SOURCE OF FUNDING NUMBERS		

10 SOURCE OF FUNDING NUMBERS			
PROGRAM ELEMENT NO	PROJECT NO	TASK NO	WORK UNIT ACCESSION NO
62301E	4506	18	05

11 TITLE (Include Security Classification)

COMPARISON OF MODAL TO NODAL APPROACHES FOR WAVEFRONT CORRECTION

12 PERSONAL AUTHOR(S)
Dr. Donald W. Hanson, Sam E. Fragapane Jr.

13a TYPE OF REPORT	13b TIME COVERED		14 DATE OF REPORT (Year, Month, Day)	15 PAGE COUNT
In-House	FROM	TO	February 1986	36

16 SUPPLEMENTARY NOTATION

N/A

17	COSATI CODES		18 SUBJECT TERMS (Continue on reverse if necessary and identify by block number)	
FIELD	GROUP	SUB GROUP	optical wavefronts	nodal wavefront correction
20	06		adaptive optical system	modal wavefront correction
			Zernike polynomials	

19 ABSTRACT (Continue on reverse if necessary and identify by block number)

The turbulent atmosphere aberrates optical wavefronts as they propagate through it. These aberrations are responsible for limiting the performance of large aperture ground based optical systems. The issue of whether to implement nodal or modal influence functions to perform wavefront correction in an adaptive optical system is studied.

Theoretically, modal wavefront correction is simpler to implement than nodal wavefront correction. This is true for very low mode aberrations, (e.g., tilt, focus). However, for large aperture, visible wavelength, adaptive optical imaging systems the number of modes which are required to be corrected becomes very high. Consequently, for these systems, nodal wavefront correction is more easily implemented.

20 DISTRIBUTION/AVAILABILITY OF ABSTRACT	21 ABSTRACT SECURITY CLASSIFICATION	
☒ UNCLASSIFIED/UNLIMITED ☐ SAME AS RPT ☐ DTIC USERS	UNCLASSIFIED	
22a NAME OF RESPONSIBLE INDIVIDUAL Sam E. Fragapane Jr.	22b TELEPHONE (Include Area Code) (315) 330-4482	22c OFFICE SYMBOL RADC (OCSP)

DD FORM 1473, 84 MAR   83 APR edition may be used until exhausted   SECURITY CLASSIFICATION OF THIS PAGE

All other editions are obsolete   UNCLASSIFIED

ACKNOWLEDGEMENTS

TABLE OF CONTENTS

LIST OF FIGURES

LIST OF TABLES

LIST OF GRAPHS

I. INTRODUCTION

Optical wavefronts are aberrated as they propagate through the turbulent atmosphere. These aberrations limit the performance of large aperture ground based optical systems. Adaptive optical systems, which measure and correct the atmospherically induced aberrations in real time, can significantly improve the performance of ground-based, large-aperture optical systems. The key components of an adaptive optical system are the wavefront sensor, which measures the aberrations, and the wavefront corrector, (e.g., deformable mirror) the figure of which is adjusted to compensate for the aberrations induced by the atmosphere. Since the earliest days of adaptive optics research there has been debate over whether the desired figure on the wavefront corrector should be implemented with nodal (i.e., local) or modal (i.e.,global) influence functions. The objective of this paper is to compare nodal and modal wavefront correction.

In the next section a discussion of the attributes of Zernike polynomials is presented. In the third section we review the concepts of nodal versus modal correction. Following that, the analyses used to compare the performance of nodal and modal wavefront correctors are presented. The results are presented in section 5 in the form of plots which compare the performance of the two approaches as a function of various parameters. We conclude with observations on the feasibility of implementing either nodal or modal correction for cases of interest.

II. ATTRIBUTES OF NODAL AND MODAL CORRECTION

From a theoretical aspect, nodal and modal correction are very similiar. The wavefront error, ϕ_e for either approach can be written as:

$$\phi_e(\vec{r}) = \phi(\vec{r}) - \phi_c(\vec{r}) \tag{1}$$

where: $\vec{r}$ is the coordinate in the aperture plane,

$\phi(\vec{r})$ is the abberation to be corrected and,

$\phi_c(\vec{r})$ is the implemented wavefront correction.

To implement a nodal correction, the wavefront to be corrected is decomposed using a basis which is determined by the nodal (actuator) influence function of the wavefront corrector. This decomposition results in a set of coefficients which correspond to the drive signal required at the corresponding node to implement the desired correction. The coefficients are typically chosen to minimize the mean square error between the aberrated wavefront and the implemented correction.

For modal correction, the wavefront is decomposed into various modes. In this paper the Zernike polynomials will be used as the basis for the decomposition. As for the nodal case, the decomposition results in a set of coefficients such that each coefficient corresponds to the strength of a particular node which is contained in the aberrated wavefront. As before, the coefficients are typically chosen to minimize the mean square error between the aberrated wavefront and the implemented correction.

Hence, for both nodal and modal correction, the following equation for mean square error averaged over the aperture, σ_e^2, is used to measure how good the correction is:

$$\sigma_e^2 = \left\langle \int W(\vec{r}) \, \phi_e^2(\vec{r}) \, dr \right\rangle \tag{2}$$

where: $W(\vec{r})$ is a window function which defines the aperture of

the wavefront corrector, and

$$W(\vec{r}) = \begin{cases} 1 \text{ inside the aperture} \\ 0 \text{ outside the aperture} \end{cases} \text{ and,} \tag{3}$$

the $\langle \ \rangle$ brackets indicate an ensemble average.

A mathematical description of a nodal correction is given below:

$$\phi_c(\vec{r}) = \sum_{i=1}^{i=N} a_i \ p(\vec{r} - \vec{r}_i) \tag{4}$$

where: a_i is the drive signal applied at location $\vec{r}_i$ and, $p(r)$ is the influence function of the wavefront corrector. (Implicit here is the assumption that the influence function is the same for every node, which is generally the case).

Using equation (4) in equation (1) and the result in equation (2) gives the residual mean square error for nodal correction, σ_{Ne}^2.

$$\sigma_{Ne}^2 = \langle \int W(\vec{r}) \ [\ \phi(\vec{r}) - \sum_{i=1}^{N} a_i \ p(\vec{r} - \vec{r}_i) \ ]^2 \ d\vec{r} \ \rangle \tag{5}$$

The error given by equation (5) can be set to any desired level by selecting the proper number of nodes. In general, the greater the number of nodes, the lower the residual error will be for a particular $W(r)$.

- 6 -

The relationship between residual error and the number of nodes will be put on a sound mathematical framework in section 4.

The residual mean square error for a modal corrector, σ^2_{Me}, is shown below:

$$\sigma^2_{Me} = \langle \int W(\vec{r})[\,O(\vec{r}) - \sum_{j=1}^{m} b_j Z_j(\vec{r})\,]^2\, d\vec{r} \rangle \qquad (6)$$

where: $Z_j(r)$ is the jth mode Zernike polynomial (defined below)
and b_j is the strength of the jth mode.

In general, the greater the number of modes which are corrected, the smaller the residual error will be. The desired residual error can be achieved by proper selection of the modes which are implemented in the wavefront corrector. This relationship will be presented in a mathematical form in section 4.

As shown in equations 5 and 6, the theoretical performance of both nodal and modal correctors is the same (i.e., any level of residual error can be obtained if enough nodes or modes are used in the wavefront corrector). The essence of the debate between the use of nodal or modal correction is thus the ease with which the desired correction can be implemented.

Conceptual one dimensional nodal and modal wavefront correctors are shown in figures 2-1 and 2-2. Nodal correction implies a local deformation of the surface of the corrector as a result of the application of a drive signal; modal correction implies a global deformation of the surface as a result of

the application of a drive signal. The conjecture which is often made is that the number of drive signals required for a modal corrector could be less than the number of drive signals required for a nodal corrector. In the following, we investigate whether, for atmospherically induced aberrations, it is likely that modal correction will require fewer drive signals than a nodal corrector.
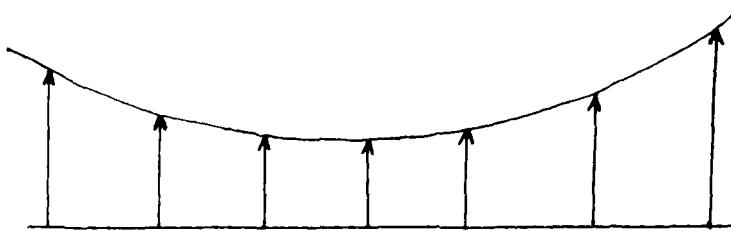
Figure 2-1. Conceptual Nodal Wavefront Corrector
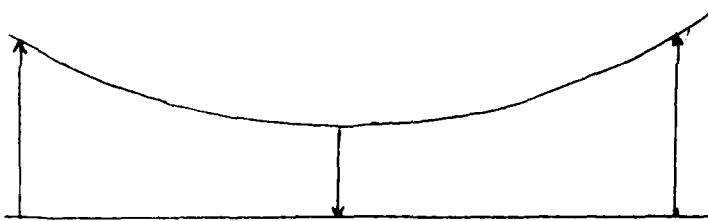
Figure 2-2. Conceptual Modal Wavefront Corrector

III. PROPERTIES OF ZERNIKE POLYNOMIALS

Zernike polynomials, or Zernike radial polynomials, are a set of polynomials which are defined on a unit circle. They are a special case of Jacobi hypergeometric polynomials which are used to establish a base set of two-dimensional polynomials that can form a polynomial function which is a product of both a purely radial and purely angular function [1]. The purely radial function, $R(r)$, describes how the surface changes from

the center to the edge of the circular aperture and the purely angular

function, $Q(\theta)$, describes how the surface changes while moving azimuthally

around the aperture. Since most optical systems have circular apertures,

Zernike polynomials provide an effective way of expressing phase

aberration over these apertures.

Zernike polynomials are conveniently expressed in polar coordinates and

can be symbolized as $R_n^m(r)$ where n is the highest power of r, or radial

degree and m is the azimuthal frequency, or angular order for which the

angular function repeats itself. Table 3-1 shows the first 19 Zernike

polynomials expressed in both polar and cartesian coordinate systems [2].

The polynomials are defined here by [3]:

$$
\left.
\begin{array}{l}
\text{a) } Zeven_j = \sqrt{n+1}\; R_n^m(r)\sqrt{2}\cos(m\theta) \\[2em]
\text{b) } Zodd_j = \sqrt{n+1}\; R_n^m(r)\sqrt{2}\sin(m\theta)
\end{array}
\right\} \qquad m = 0 \qquad (7)
$$

$$
\left.
Z_j = \sqrt{n+1}\; R_n^0(r)
\right\} \qquad m = 0 \qquad (8)
$$

$$
\text{where: } \quad R_n^m(r) = \sum_{s=0}^{(n-m)/2} \frac{(-1)^s\,(n-s)!}{s!\,[(n+m)/2 - s]!\,[(n-m)/2 - s]!}\; r^{n-2s} \qquad (9)
$$

The index j is a mode ordering number and the values of n and m are always

integers which satisfy $m < n$, and $n - m$ = even. Consequently, only

polynomials with certain combinations of n and m exist (see table 3-2) [3].

n	R_n^m	$R(r,\theta)$	$R(x,y)$
(1)	R_1^1	$r \cos\theta$	x
(2)	R_1^{-1}	$r \sin\theta$	y
(3)	R_2^0	$2r^2-1$	$2x^2+2y^2-1$
(4)	R_2^2	$r^2 \cos2\theta$	x^2-y^2
(5)	R_2^{-2}	$r^2 \sin2\theta$	$2xy$
(6)	R_3^1	$(3r^2-2)r \cos\theta$	$3x^3+3xy^2-2x$
(7)	R_3^{-1}	$(3r^2-2)r \sin\theta$	$3x^2y+3y^3-2y$
(8)	R_4^0	$6r^4-6r^2+1$	$6x^4+12x^2y^2 +6y^4-6x^2-6y^2+1$
(9)	R_3^3	$r^3 \cos3\theta$	x^3-3xy^2
(10)	R_3^{-3}	$r^3 \sin3\tau$	$3x^2y-y^3$
(11)	R_4^2	$(4r^2-3)r^2 \cos2\theta$	$4x^4-3x^2+3y^2-4y^4$
(12)	R_4^{-2}	$(4r^2-3)r^2 \sin2\theta$	$8x^3y+8xy^3-6xy$
(13)	R_5^1	$(10r^4-12r^2+3)r \cos\theta$	$10x^5+20x^3y^2+10xy^4-12x^3-12xy^2+3x$
(14)	R_5^{-1}	$(10r^4-12r^2+3)r \sin\theta$	$10x^4y+20x^2y^3+10y^5-12x^2y-12y^3+3y$
(15)	R_6^0	$20r^6-30r^4+12r^2-1$	$20x^6+60x^4y^2+60x^2y^4+20y^6-30x^4$ $-60x^2y^2-30y^4+12x^2+12y^2-1$
(16)	R_4^4	$r^4 \cos4\theta$	$x^4-6x^2y^2+y^4$
(17)	R_4^{-4}	$r^4 \sin4\theta$	$4x^3y-4xy^3$
(18)	R_5^3	$(5r^2-4)r^3 \cos3$	$5x^5-10x^3y^2-4x^3-15xy^4+12xy^2$
(19)	R_5^{-3}	$(5r^2-4)r^3 \sin3$	$-5y^5+10x^2y^3+4y^3+15x^4y-12x^2y$

Table 3-1

Table 3-2

| RADIAL degree (n)	Azimuthal frequency (m)					
	0	1	2	3	4	5
0	$z_1=1$ Constant					
1		$z_2=2r\cos\theta$ $z_3=2r\sin\theta$ Tilts (Lateral position)				
2	$z_4=3(2r^2-1)$ Defocus (Longitudinal position)		$z_5=6r^2\sin2\theta$ $z_6=6r^2\cos2\theta$ Astigmatism (3rd Order)			
3		$z_7=8(3r^3-2r)\sin\theta$ $z_8=8(3r^3-2r)\cos\theta$ Coma (3rd order)		$z_9=8r^3\sin3\theta$ $z_{10}=8r^3\cos3\theta$		
4	$z_{11}=5(6r^4-6r^2+1)$ 3rd order spherical		$z_{12}=10(4r^4-3r^2)\cos2\theta$ $z_{13}=10(4r^4-3r^2)\sin2\theta$		$z_{14}=10r^4\cos4\theta$ $z_{15}=10r^4\sin4\theta$	
5		$z_{16}=12(10r^5-12r^3+3r)\cos\theta$ $z_{17}=12(10r^5-12r^3+3r)\sin\theta$		$z_{18}=12(5r^5-4r^3)\cos3\theta$ $z_{19}=12(5r^5-4r^3)\sin3\theta$		$z_{20}=12r^5\cos5\theta$ $z_{21}=12r^5\sin5\theta$
6	$z_{22}=7(20r^6-30r^4+12r^2-1)$ 5th order spherical		z_{23} z_{24}		z_{25} z_{26}	

As mentioned earlier, Zernike polynomials are particularily valuable for their unique properties over a circular aperture. Also, they are extremely valuable due to their relationship to classical aberrations. Therefore, they provide a convenient mathematical expression of the aberrating content in a wavefront using familiar terms (see figures 3-1 through 3-6) [4].

The properties posessed by the Zernike radial polynomials over a circular aperture are enumerated below [2]:

(1) They are orthogonal over the unit circle.

(2) They are normalized.

(3) In the term $R_n^m(r)$, if m is even n must be even,

and if m is odd n must be odd.

(4) The term $R_n^m(r)$ contains no power of r less than m
(i.e. $n > m$).

As described above, Zernike polynomials possess several properties which make them ideally suited for describing the aberrations present in an optical system. From (1), one of their most important properties is that they form an orthogonal set of polynomials over a normalized circular aperture. This implies that each term is independent from all others. Consequently, varying one term in the series will not effect the values of the other terms. This characteristic is extremely important in the process of correcting an atmospherically induced aberrated wavefront in an adaptive optical system. Lastly, each term of the set of Zernike polynomials can be related to another set of deformations of the lowest order called the Seidal aberrations [2].
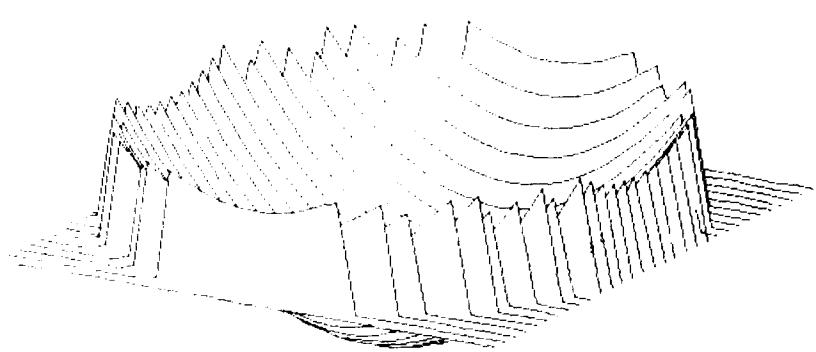
- 12 -
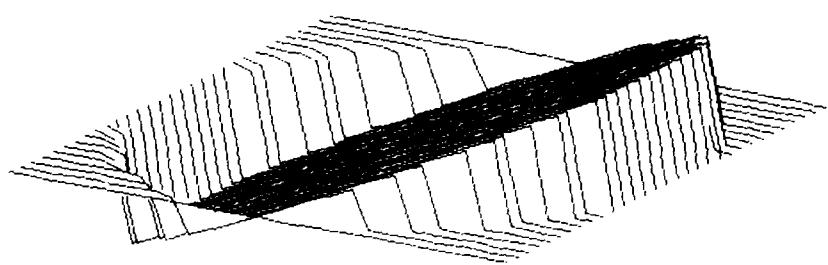
TILT ZERNIKE POLYNOMIAL

Figure 3-1a
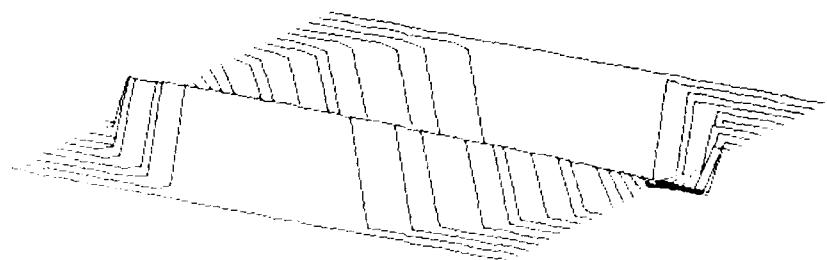
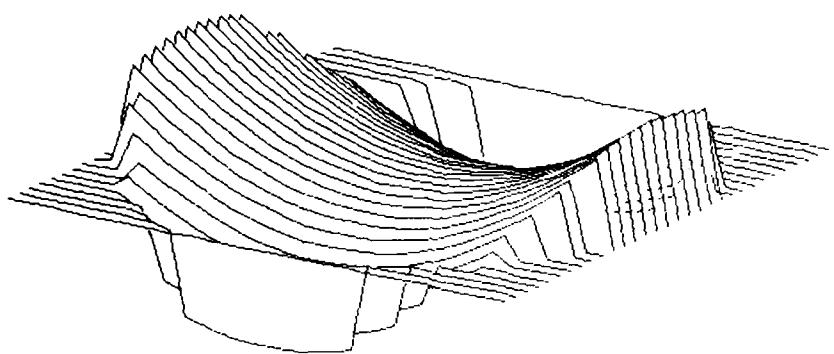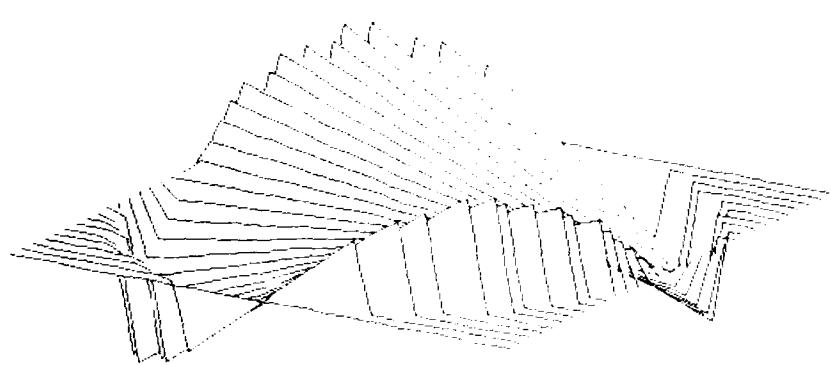TILT ZERNIKE POLYNOMIAL

Figure 3-1b
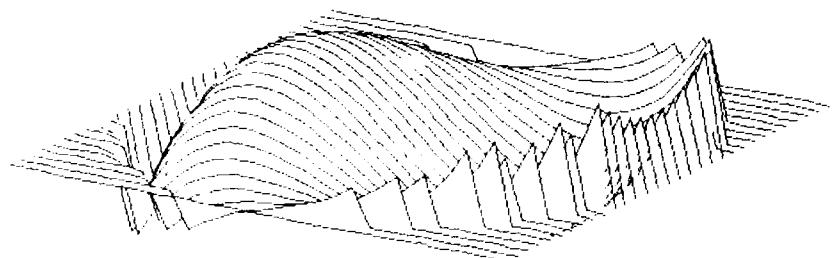
DEFOCUS ZERNIKE POLYNOMIAL

Figure 3-2

ASTIGMATISM ZERNIKE POLYNOMIAL

Figure 3-3a
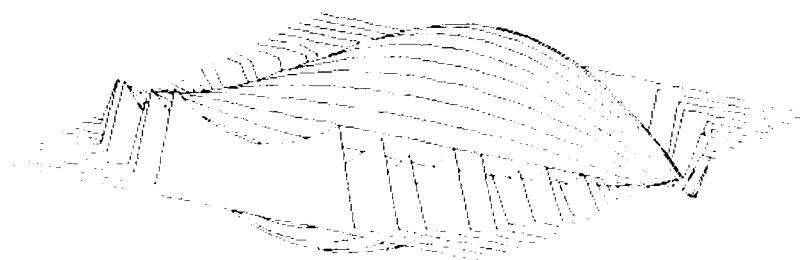
ASTIGMATISM ZERNIKE POLYNOMIAL

Figure 3-3b

-15-

COSH ZERNIKE POLYNOMIAL
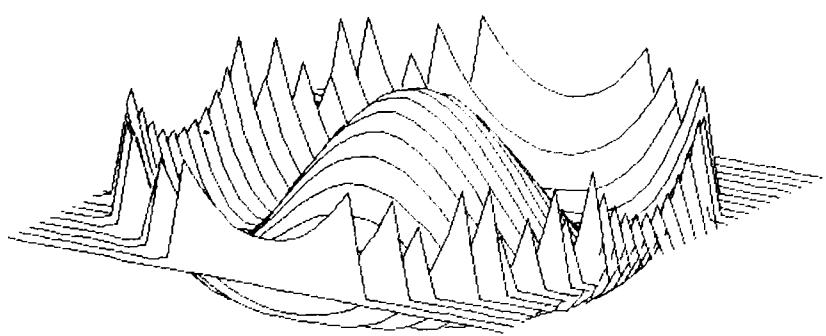
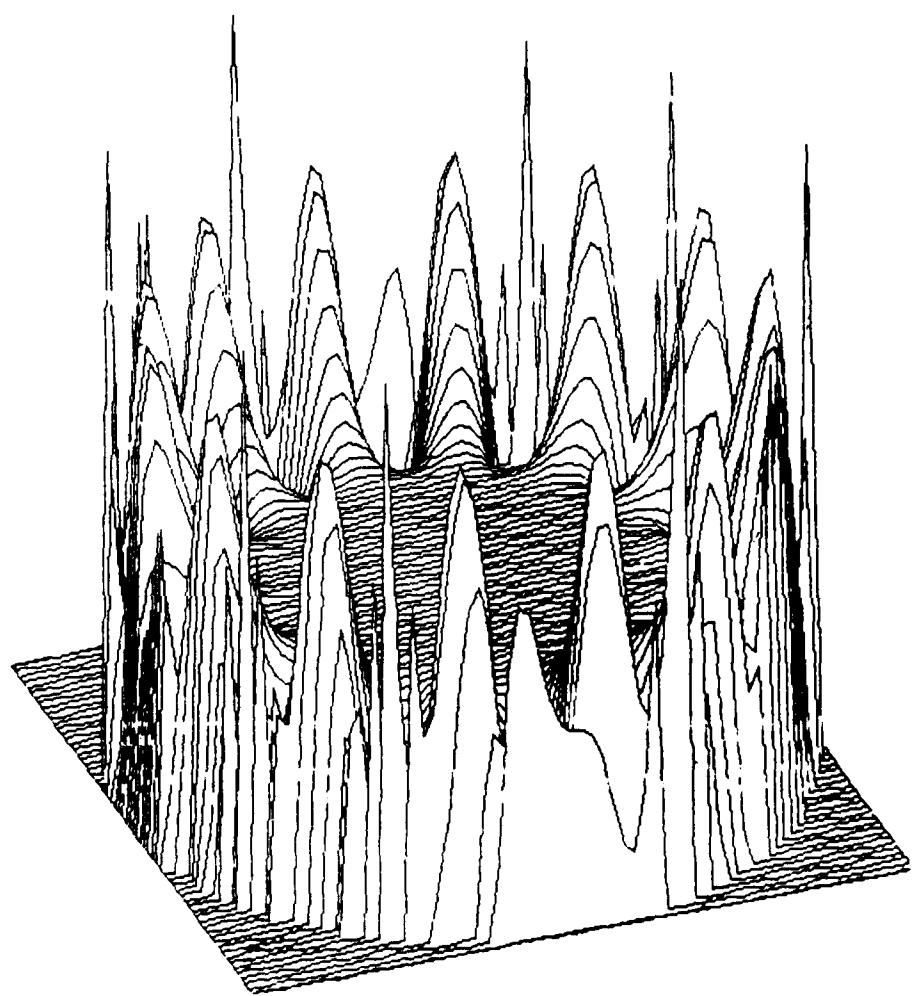Figure 3-4a

Figure 3-4b

SPHERICAL ZERNIKE POLYNOMIAL

Figure 3-5

151st Zernike Polynomial

Figure 3-6

Figures 3-1 through 3-5 shows the first five lower order Zernike polynomials which represent classical aberrations. Figure 3-6 shows a higher order polynomial.

| ZERNIKE POLYNOMIALS | | | | | |
| FIGURES WITH COEFFICIENTS | | | | | |
Figure		Name	Figure		Name
3-1)	a.	Tilt	3-4)	a.	Coma
	b.			b.	
3-2)		Defocus	3-5)		Spherical
3-3)	a.	Astigmatism	3-6)		151st Zernike Polynomial
	b.				

Table 3-3

IV. MODAL TO NODAL COMPARISION

In this section we compare the number of drive siginals required for the nodal and modal methods to implement a wavefront correction which equally compensates for atmospherically induced wavefront deformations.

The equation for the mean square residual error of the wavefront using nodal correction is defined here by [5]:

$$\sigma_{Ne}^2 = a \, (d/r_o)^{5/3} \quad [\text{rad}^2] \qquad (10)$$

where: σ_{Ne}^2 is the mean square residual error of the wavefront.

a is a constant which depends on the wavefront corrector (.141 < a < .34)

- 19 -

d is the spacing between actuators in the wavefront corrector, and

r_o is the phase coherence length of the atmosphere.

The equation for the residual error of the wavefront using modal correction is defined here by [3]:

$$\sigma^2_{Me} = .2944 J^{-\sqrt{3}/2} (D/r_o)^{5/3} \quad [rad^2] \qquad (11)$$

where: σ^2_{Me} is the mean square residual error of the wavefront.

J is the number of modes.

D is the diameter of the aperture.

r_o is the phase coherence length of the atmosphere.

The two methods of wavefront correction were compared to one another by plotting various parameters of the two equations. The series of four graphs developed for the comparison will be discussed here. The analysis and results of this graphical comparison will be presented in the next section.

OBSERVATIONS FROM GRAPH 4-1

The first graph (graph 4-1) is a plot of the mean square residual error for modal correction versus the number of modes (J). σ^2_{Me} was calculated from equation (11) for values of D/r_o shown.

This graph shows the number of modes (J) necessary to achieve a given mean square residual error. For each of the four cases of D/r_o = 10, 20, 50, and 100, the plots are exponential and show that as the number of modes (J)

increases, the residual error squared (σ^2_{Me}) decreases and conversely, J decreases as σ^2_{Me} increases. Therefore, the greater the number of modes corrected, the less the wavefront error will be.

Further observation shows that as the ratio of the diameter of the aperture to the phase coherence length of the atmosphere (D/r_o) increases, the number of modes (J) necessary to obtain an acceptably small wavefront error rapidly increases. Consequently, in order to achieve the image quality desired in an optical system, the number of mode corrections necessary may be very high for the D/r_o of useful systems.

OBSERVATIONS FROM GRAPH 4-2

The second graph (graph 4-2) is a plot of the mean square residual error for nodal correction versus the actuator spacing divided by the phase coherence length of the atmosphere (d/r_o). σ^2_{Ne} was calculated from equation 10 for a = 0.2, 0.4, and 1.0 at values of d/r_o = 0.2, 0.5, 1.0, and 2.0. Each of the 3 plots contains 4 data points.

Each of the three plots is exponential in shape and indicates that as d/r_o increases, the residual error of the wavefront also increases. In addition, analysis of the three plots indicates that as the parameter (a) increases, the larger σ^2_{Ne} becomes for a given value of d/r_o. This observation follows from the nodal equation (1) seeing that the term (a) acts as a multiplication factor.
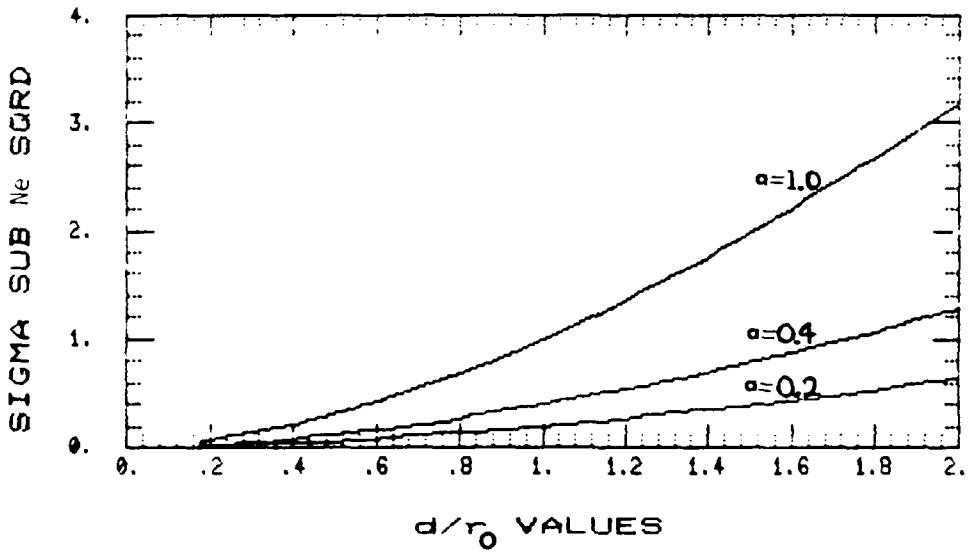
Further observation of the 3 plots suggests that the implementation

Mean square residual error as a function of the number of modes
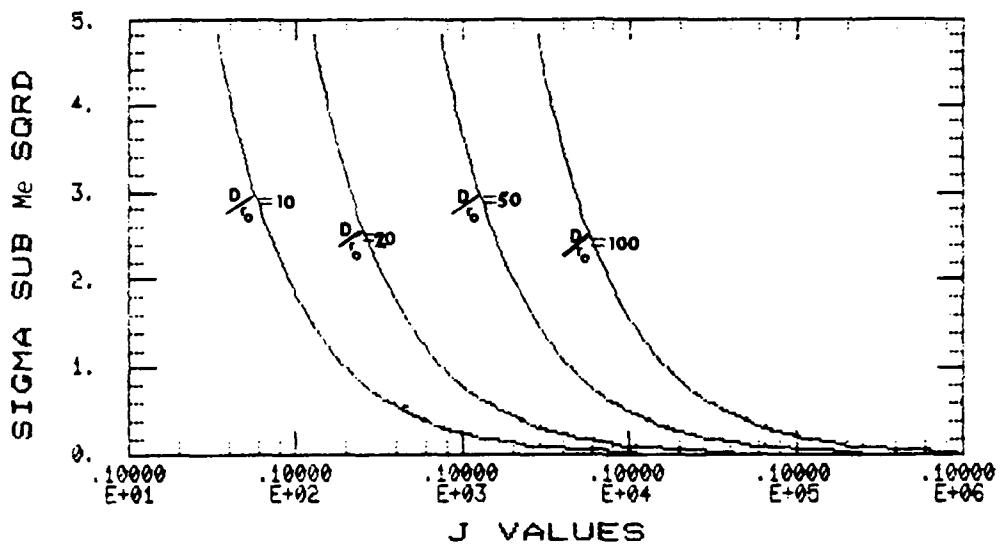
Graph 4-1

Residual error squared as a function of the spacing between the
actuators in the wavefront corrector divided by the phase
coherence length of the atmosphere

Graph 4-2

of a nodal wavefront corrector in a compensated imaging system can achieve an acceptable mean square wavefront error of 0.6 rad^2, for a relatively large d/r_0 (equal to approximately 2.0) and a value of the parameter (a) equal to 0.2.

OBSERVATIONS FROM GRAPH 4-3

The third graph (graph 4-3) is a plot of (d/r_0) verses the number of modes (J) for the case where $\sigma^2_{Me} = \sigma^2_{Ne}$. σ^2_{Ne} was calculated from equation 10, for a = 0.2 and d/r_0 = 0.2 to 2.0 in 0.2 increments. σ^2_{Ne} was then substituted into equation 11 with D/r_0 = 10, 20, 50, and 100 to calculate the corresponding value of J. Consequently, each of the 4 plots contains 10 data points. The d/r_0 scale is linear from 0.2 to 2.2 and the J scale is logarithmic from 1 to 1,000,000. Graph 3 provides a comparison betwee the performance of modal-to-nodal wavefront correctors.

On the x axis is the number of modes (J) which was derived from the modal equation and on the y axis is (d/r_0) which was derived from the nodal equation (10). Graph 4-3 contains 4 plots, for D/r_0 = 10, 20, 50, and 100, which are exponential in shape. From the four curves, it is observed that the greater the number of modes (J), the smaller d/r_0 must be to provide the same performance of the wavefront corrector. For a residual error of the wavefront specified by a given value of d/r_0, the greater D/r_0 becomes, the greater the number of modes necessary to achieve this σ^2_e.

Using the relationship

$$N = (D/d)^2 \qquad (12)$$

where: N is equal to the number of nodes.

A direct comparison can be made between the number of nodes (N) to the number of modes (J) necessary to achieve a given residual error of the wavefront. Solving (12) for d gives:

$$d = D/\sqrt{N} \tag{13}$$

Using (13) in (10) gives :

$$\sigma^2_{Ne} = a \left(\frac{D/\sqrt{N}}{r_o} \right)^{5/3} \tag{14}$$

$$= a \, N^{-5/6} \, (D/r_o)^{5/3} \tag{15}$$

Equating (15) and (11) gives:

$$a \, N^{-5/6} \, (D/r_o)^{5/3} = .2944 \, J^{-\sqrt{3}/2} \, (D/r_o)^{5/3} \tag{16}$$

solving for N and simplifing gives:

$$N = 4.338 \, a^{6/5} \, J^{1.04} \tag{17}$$

A plot of this function is shown in graph 4-4.

Using the above we can finally compare the feasibility of using nodal verses modal correction for atmospheric turbulence. To make the comparison we use a hypothetical adaptive optical system which has a diameter, D, of 2 meters. We assume, based on measurements, an atmospheric coherence length, r_o, of 10 cm. Based on measured data, a reasonable value for the parameter (a) is 0.2. We select σ^2_{Ne} = 0.561 rad^2 as a r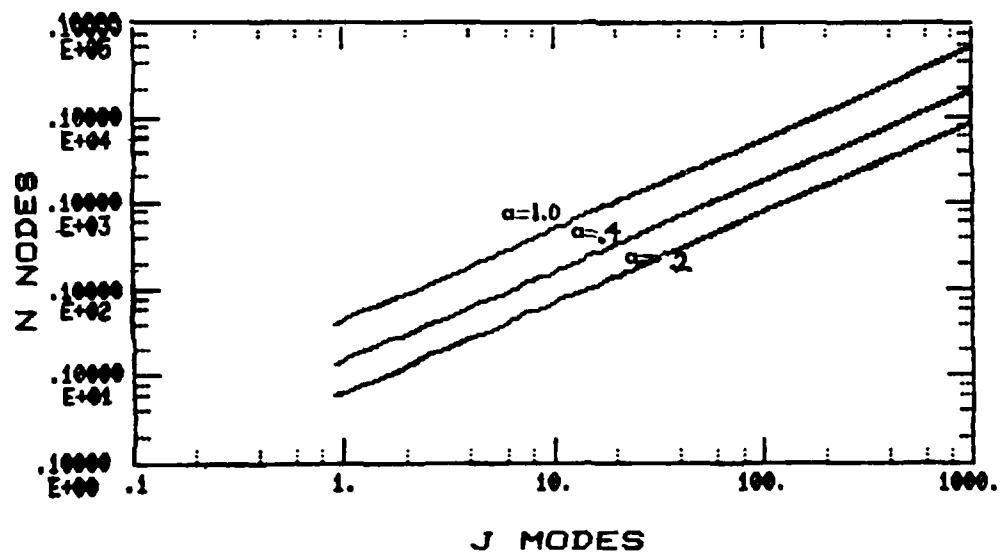easonable residual wavefront error. Using the above values for D, r_o, σ^2_{Ne} and a in (15) gives an N of 116.

- 24 -

The spacing between the actuators in the wavefront corrector
divided by the phase coherence length of the atmosphere as a
function of the number of modes
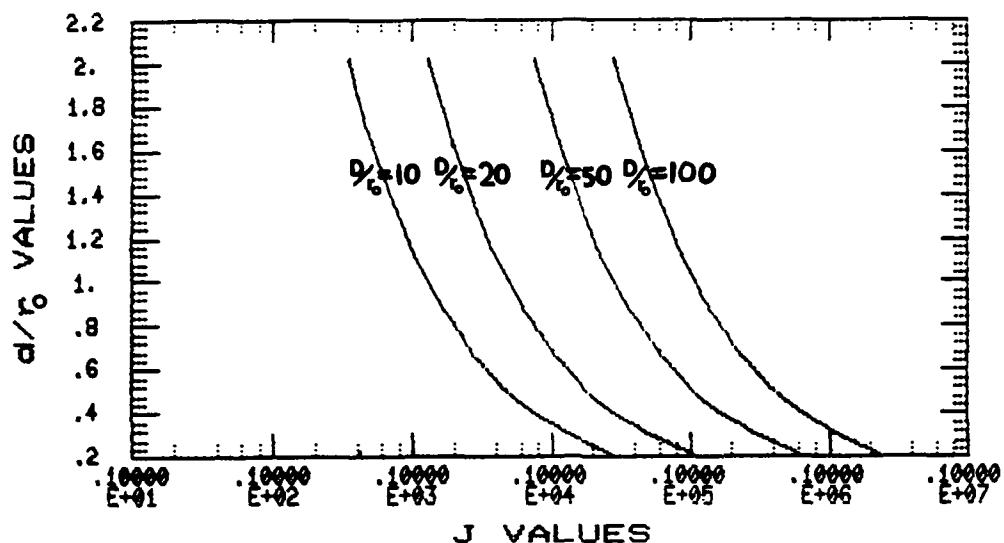
Graph 4-3

The number of nodes as a function of the number of modes

Graph 4-4

Substituting this value of N into (17) gives 151 for a value of J. A plot of this Zernike polynomial is shown in figure 3-6. It would appear that many actuators would be required to implement this mode. The data from the comparison done on graph 4-3 is shown in table 4-1.

NUMBER OF NODES TO NUMBER OF MODES COMPARISON

| d/r_o	D/r_o	10	20	50	100
.2	N	2,239	10,036	63,673	258,453
	J	2,600	11,000	65,000	250,000
1.0	N	107	386	2,239	10,036
	J	140	480	2,600	11,000
2.0	N	25	107	606	2,239
	J	35	140	740	2,600

Table 4-1

From table 4-1 it can be seen that the number of nodes (N) increases for a given d/r_o and larger values of D/r_o. This was also the case for the number of modes J as was stated earlier. Overall, the number of modes is approximately the same as the number of nodes for producing a particular residual error of the wavefront for all combinations of d/r_o and D/r_o. Consequently, an atmospheric modal wavefront corrector will require more actuators than a nodal corrector to compensate for a heavily aberrated wavefront in a large aperture ground-based optical system, since each mode will require several actuators.

V. CONCLUSION

In theory modal correction systems are simpler to implement than nodal correction systems. For very low mode aberrations, (e.g.,tilt,focus) modal corrections show that this simplification can be realized. However, for large aperature, visible wavelength, adaptive optical imaging systems the number of modes which are required to be corrected becomes very high. Implementation of each of these modes with only a few actuators does not seem practical. Therefore, for such systems, nodal wavefront correctors are the wavefront corrector of choice.

VI. REFERENCES

[1] M. Born and F. Wolf, <u>Principles of Optics</u>, (Pergamer Press Ltd., New York, 1965).

[2] D. Anderson, "Fringe Manual," Optical Sciences Center, University of Arizona (April 1982).

[3] R. J. Noll, "Zernike Polynomial and Atmospheric Turbulence," J. Opt. Soc. Am. 66, 207-211 (1976).

[4] J. Y. Wang and D. E. Silva, "Wave-front Interpretation with Zernike Polynomials," <u>Applied Optics</u>, <u>19</u>, 9 (1980).

[5] D. P. Greenwood and D. L. Fried, "Power Spectra Requirements for Wave-Front Compensative Systems," J. Opt. Soc. Am. 66, 193-206 (1976).
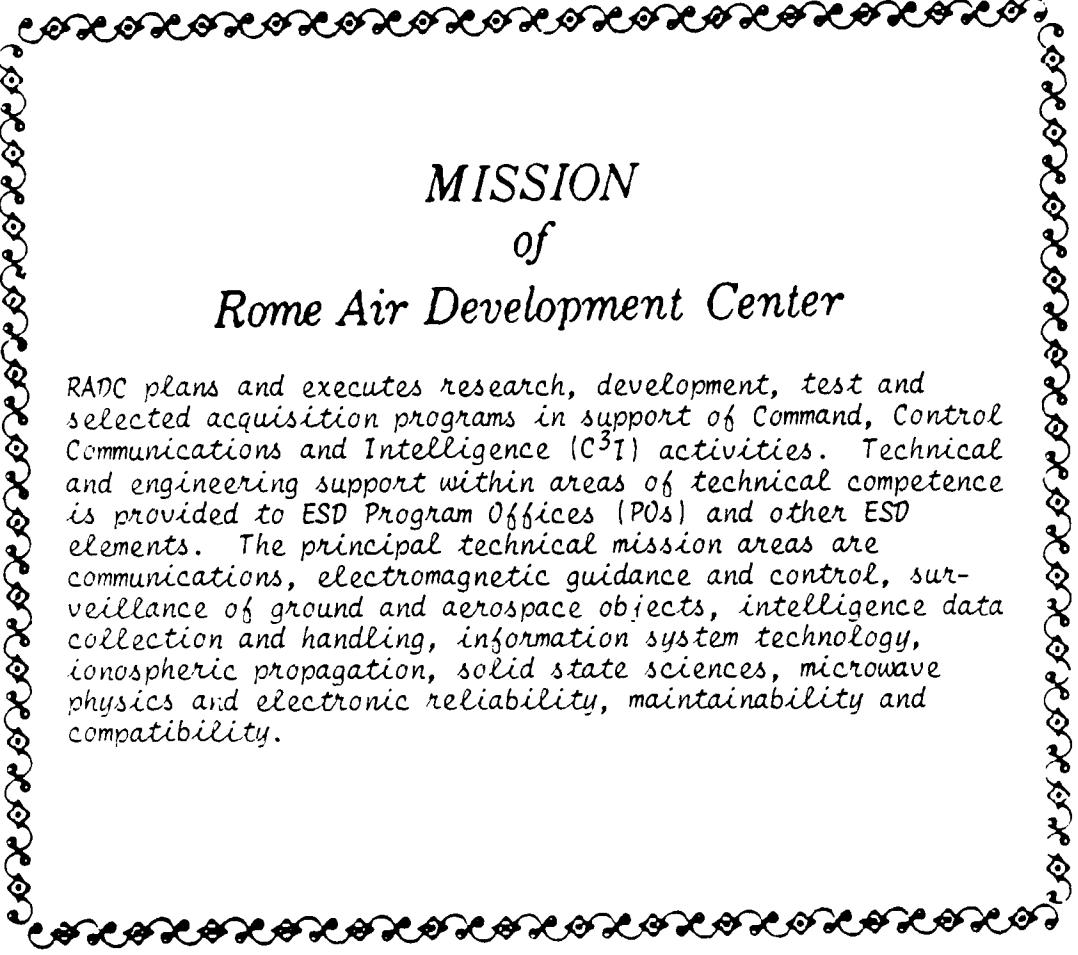
MISSION
of
Rome Air Development Center

RADC plans and executes research, development, test and selected acquisition programs in support of Command, Control Communications and Intelligence (C^3I) activities. Technical and engineering support within areas of technical competence is provided to ESD Program Offices (POs) and other ESD elements. The principal technical mission areas are communications, electromagnetic guidance and control, surveillance of ground and aerospace objects, intelligence data collection and handling, information system technology, ionospheric propagation, solid state sciences, microwave physics and electronic reliability, maintainability and compatibility.

END

DTIC

6-86